JOC Article

Thermal Isomerization of Tricyclo[4.1.0.0^{2,7}]heptane and Bicyclo[3.2.0]hept-6-ene through the (*E*,*Z*)-1,3-Cycloheptadiene Intermediate

Changyong Qin and Steven R. Davis*

Department of Chemistry and Biochemistry, University of Mississippi, University, Mississippi 38677

davis@chemistry.olemiss.edu

Received August 8, 2003

The thermal isomerization of tricyclo[4.1.0.0^{2,7}]heptane and bicyclo[3.2.0]hept-6-ene was studied using ab initio methods at the multiconfiguration self-consistent field level. The lowest-energy pathway for thermolysis of both structures proceeds through the (*E*,*Z*)-1,3-cycloheptadiene intermediate. Ten transition states were located, which connect these three structures to the final product, (*Z*,*Z*)-1,3-cycloheptadiene. Three reaction channels were investigated, which included the conrotatory and disrotatory ring opening of tricyclo[4.1.0.0^{2,7}]heptane and bicyclo[3.2.0]hept-6-ene and trans double bond rotation of (*E*,*Z*)-1,3-cycloheptadiene. The activation barrier for the conrotatory ring opening of tricyclo[4.1.0.0^{2,7}]heptane to (*E*,*Z*)-1,3-cycloheptadiene was found to be 40 kcal mol^{-1}, while the disrotatory pathway to (*Z*,*Z*)-1,3-cyclohetpadiene was calculated to be 55 kcal mol^{-1}. The thermolysis of bicyclo[3.2.0]hept-6-ene via a conrotatory pathway to (*E*,*Z*)-1,3-cycloheptadiene had a 35 kcal mol^{-1} barrier, while the disrotatory pathway to (*Z*,*Z*)-1,3-cyclohetpadiene had a barrier of 48 kcal mol^{-1}. The barrier for the isomerization of (*E*,*Z*)-1,3-cycloheptadiene to bicyclo[3.2.0]hept-6-ene was found to be 12 kcal mol^{-1}, while that directly to (*Z*,*Z*)-1,3-cycloheptadiene was 20 kcal mol^{-1}.

Introduction

The thermal isomerization of tricyclo[4.1.0.0^{2,7}]heptane (**1**) was initially reported by Wiberg and Szeimies[1] who studied the thermolysis in the gas phase in which a mixture of bicyclo[3.2.0]hept-6-ene (**2**) and (*Z*,*Z*)-1,3-cycloheptadiene (**3**) resulted. The proportion of **3** in the product decreased as the thermolysis temperature decreased, prompting the authors to infer that **3** must be formed from **2**. One of the most interesting suggestions was that the reaction of **1** proceeded through the (*E*,*Z*)-1,3-cycloheptadiene intermediate (**4**) following an allowed conrotatory process. Christl et al.[2] measured an activation energy of the **1** → **2** thermolysis in solution of 38 kcal mol^{-1} but had a mixture of 40% **2** and 60% 2-norcarene as products. In a later paper, Christl et al.[3] argued that the conversion of **1** to **2** followed a concerted but highly asynchronous pathway to the intermediate **4** and then underwent a rapid conrotatory ring closure to give **2**. The activation energy was measured in solution to be 37.6 kcal mol^{-1} under conditions that gave a virtually quantitative yield of **2** as the only product. The study by Branton et al.[4] confirmed that product **3** results from **2**, in which it was reported that the thermal isomerization of **2** gave **3** as the only product. The activation energy was measured to be 45 kcal mol^{-1}, and the reaction was suggested to proceed through a concerted pathway. However, the authors dismissed the possibility of the reaction including the intermediate **4** on the basis of its perceived strain energy. We have shown the six-membered ring (*E*,*Z*)-1,3-cyclohexadiene to be an intermediate in the thermolysis of tricyclo[3.1.0.0^{2,6}]hexane;[5] therefore the larger seven-carbon ring **4** would be expected to also be a viable intermediate for the isomerization of **1**. An even more interesting question is whether **2** also thermolyzes through the intermediate **4**, and if so, what are the relative activation barriers for the **4** → **2** and **4** → **3** reactions? In this paper we will report the results of an investigation of the possible thermolysis pathways of **1** and **2** and the role of the intermediate **4**.

Computational Methods

The multiconfiguration self-consistent field calculations were performed using the GAMESS[6] and Gaussian98[7] suite of programs. Geometries were optimized using the 6-31G(d,p) basis set,[8] employing analytic first derivatives, while harmonic frequencies were determined using second derivatives computed from finite differences of the analytic first derivatives. Single-point corrections to the

* Corresponding author.

(1) Wiberg, K. B.; Szeimies, G. *Tetrahedron Lett.* **1968**, *10*, 1235.

(2) Christl, M.; Heinemann, U.; Kristof, W. *J. Am. Chem. Soc.* **1975**, *97*, 2299.

(3) Christl, M.; Stangl, R.; Jelinek-Fink, H. *Chem. Ber.* **1992**, *125*, 485.

(4) Branton, G. R.; Frey, H. M.; Montague, D. C.; Stevens, R. D. R. *Trans. Faraday Soc.* **1966**, *62*, 659.

(5) Davis, S. R.; Nguyen, K. A.; Lammertsma, K.; Mattern, D. L.; Walker, J. E. *J. Phys. Chem. A* **2003**, *107*, 198.

(6) Schmidt, M. W.; Baldridge, K. K.; Boatz, J. A.; Elbert, S. T.; Gordon, M. S.; Jensen, J. H.; Koseki, S.; Matsunaga, N.; Nguyen, K. A.; Su, S. J.; Windus, T. L.; Dupuis, M.; Montgomery, J. A. *J. Comput. Chem.* **1993**, *14*, 1347.

10.1021/jo035168s CCC: $25.00
Published on Web 10/24/2003

SCHEME 1

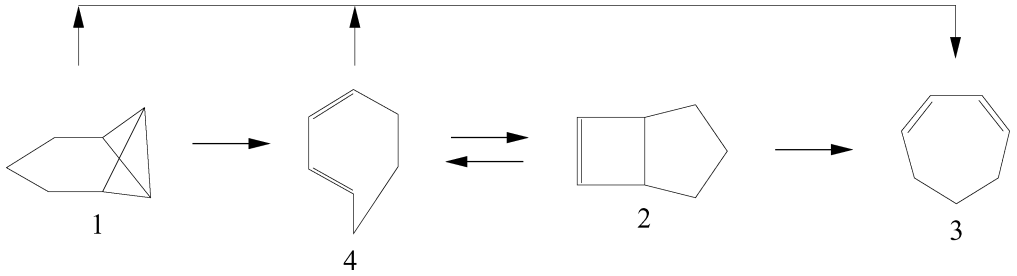

TABLE 1. Total,[a] Zero-Point,[a] and Relative Energies[b]

structure	E_{MCSCF}[c]	$E_{MCQDPT2}$[d]	ZPE[c]	$E_{rel,MCSCF}$[c]	$E_{rel,QDMCPT2}$[c]	$E_{rel,CCSD(T)}$[e]
1	−270.9527	−271.8077	0.1606	0	0	0
2	−270.9830	−271.8312	0.1600	−19.3	−15.0	−13.9
2′	−270.9774	−271.8243	0.1598	−15.9	−10.8	−10.0
3	−271.0121	−271.8452	0.1596	−37.8	−24.0	−23.4
4	−270.9517	−271.7943	0.1588	−0.4	7.4	9.7
4′	−270.9500	−271.7919	0.1587	0.7	8.9	11.2

[a] Hartrees. [b] kcal mol^{-1}. [c] MCSCF/6-31G(d,p). [d] MCQDPT2/6-31G(d,p)//MCSCF/6-31G(d,p). [e] CCSD(T)/6-31G(d,p)//MP2/6-31G(d,p).

MCSCF energies were obtained using the second-order multiconfigurational quasidegenerate perturbation theory (MCQDPT2),[9−10] also with the 6-31G(d,p) basis set. For **1**, the MCSCF active orbitals consisted of the five occupied and five virtual C−C MOs comprising the bicyclobutane moiety, namely, the C1−C2, C1−C6, C1−C7, C2−C7, and C6−C7 bonds. For the cycloheptadienes, the bonding orbitals included the C1=C2 and C6=C7 π bonds plus the C1−C7, C1−C2, and C6−C7 σ bonds, and for the bicycloheptanes, the active space consisted of the C1−C7, C1−C2, C2−C6, and C6−C7 σ bonds and the C1=C7 π bond. This gives an active space consisting of 10 electrons in 10 orbitals, MCSCF(10,10). Geometries were classified as either minima or transition states by computing the harmonic frequencies. The intrinsic reaction coordinate[11−13] was followed in both directions from each transition state to verify the connection between the reactant and product.

Results and Discussion

Relative energies for the minima and transition states are given in Tables 1 and 2, respectively, while activation barriers are listed in Table 3. It is the bicyclobutane moiety of **1** that opens during thermolysis; therefore, the thermal isomerization of bicyclobutane can be used as a model. Experimental evidence points to a concerted mechanism,[14−16] which is also supported by computational studies.[17−18] The closely related structure tricyclo-

TABLE 2. Total Energies,[a] Zero-Point Energies,[a] and Imaginary Frequencies[b]

transition state	E_{MCSCF}[c]	$E_{MCQDPT2}$[d]	ZPE[c]	imag freq[c]
TS1	−270.8840	−271.7410	0.1566	259i
TS2	−270.8812	−271.7377	0.1565	84i
TS3	−270.9155	−271.7717	0.1565	652i
TS4	−270.9144	−271.7707	0.1566	646i
TS5	−270.9132	−271.7590	0.1547	832i
TS6	−270.9084	−271.7545	0.1547	812i
TS7	−270.9030	−271.7484	0.1540	573i
TS8	−270.9008	−271.7463	0.1525	441i
TS9	−270.8643	−271.7150	0.1553	394i
TS10	−270.8616	−271.7118	0.1553	317i

[a] Hartrees. [b] cm^{-1}. [c] MCSCF/6-31G(d,p). [d] MCQDPT2/6-31G(d,p)//MCSCF/6-31G(d,p).

TABLE 3. Activation Barriers[a]

reaction	TS	$E_{a,MCSCF}$[b]	$E_{a,MCQDPT2}$[c]
1 → 4	**TS1**	40.7	39.5
1 → 4′	**TS2**	42.4	41.5
4 → 2	**TS3**	21.3	12.7
4′ → 2′	**TS4**	21.0	12.0
2 → 4	**TS3**	40.2	35.1
2′ → 4′	**TS4**	37.5	31.6
4 → 3	**TS5**	21.6	19.6
4′ → 3	**TS6**	23.6	21.0
2 → 3	**TS7**	46.4	48.2
2′ → 3′	**TS8**	43.5	45.0
1 → 3	**TS9**	52.3	55.0
1 → 3	**TS10**	54.0	57.0

[a] kcal mol^{-1}. [b] MCSCF/6-31G(d,p). [c] MCQDPT2/6-31G(d,p)//MCSCF/6-31G(d,p).

(7) Frisch, M. J.; Trucks, G. W.; Schlegel, H. B.; Scuseria, G. E.; Robb, M. A.; Cheeseman, J. R.; Zakrzewski, V. G.; Montgomery, J. A., Jr.; Stratmann, R. E.; Burant, J. C.; Dapprich, S.; Millam, J. M.; Daniels, A. D.; Kudin, K. N.; Strain, M. C.; Farkas, O.; Tomasi, J.; Barone, V.; Cossi, M.; Cammi, R.; Mennucci, B.; Pomelli, C.; Adamo, C.; Clifford, S.; Ochterski, J.; Petersson, G. A.; Ayala, P. Y.; Cui, Q.; Morokuma, K.; Malick, D. K.; Rabuck, A. D.; Raghavachari, K.; Foresman, J. B.; Cioslowski, J.; Ortiz, J. V.; Stefanov, B. B.; Liu, G.; Liashenko, A.; Piskorz, P.; Komaromi, I.; Gomperts, R.; Martin, R. L.; Fox, D. J.; Keith, T.; Al-Laham, M. A.; Peng, C. Y.; Nanayakkara, A.; Gonzalez, C.; Challacombe, M.; Gill, P. M. W.; Johnson, B. G.; Chen, W.; Wong, M. W.; Andres, J. L.; Head-Gordon, M.; Replogle, E. S.; Pople, J. A. *Gaussian 98*, revision A.11.1; Gaussian, Inc.: Pittsburgh, PA, 1998.
(8) Hehre, W. J.; Ditchfield, R.; Pople, J. A. *J. Chem. Phys.* **1972**, *56*, 2257.
(9) Nakano, H. *J. Chem. Phys.* **1993**, *99*, 7983.
(10) Nakano, H. *Chem. Phys. Lett.* **1993**, *207*, 372.
(11) Boys, S. F. *Rev. Mod. Phys.* **1960**, *32*, 296.
(12) Gonzalez, C.; Schlegel, H. B. *J. Chem. Phys.* **1989**, *90*, 2154.
(13) Gonzalez, C.; Schlegel, H. B. *J. Phys. Chem.* **1990**, *94*, 5523.
(14) Blanchard, E. P., Jr.; Carncross, A. *J. Am. Chem. Soc.* **1966**, *88*, 487.
(15) Closs, G. L.; Pfeffer, P. E. *J. Am. Chem. Soc.* **1968**, *90*, 2452.
(16) Wiberg, K. B.; Lavanish, J. M. *J. Am. Chem. Soc.* **1966**, *88*, 5272.
(17) Shevlin, P. B.; McKee, M. L. *J. Am. Chem. Soc.* **1988**, *110*, 1666.
(18) Nguyen, K. A.; Gordon, M. S. *J. Am. Chem. Soc.* **1995**, *117*, 3835.

SCHEME 2

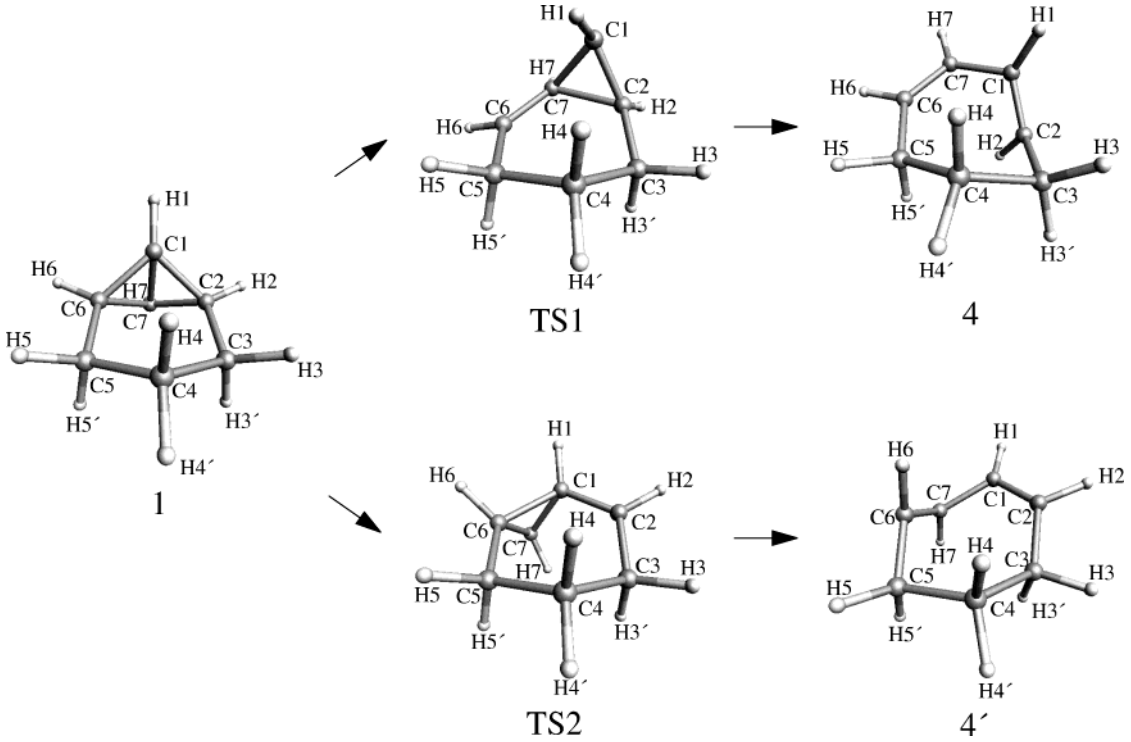

[3.1.0.0^{2,6}]hexane[5] also follows a concerted, asynchronous pathway through cleavage of two opposing bonds in the bicyclobutane moiety. For **1**, the opposing bonds comprise either C1−C2 and C6−C7 or C1−C6 and C2−C7. Two possibile pathways are expected; the conversion directly to **3** follows a disrotatory path, or the formation of intermediate **4** occurs through a conrotatory process. Since **1** belongs to point group C_s, the C1−C2 and C6−C7 bonds are not equivalent; therefore, the barrier is expected to depend on which bond breaks first in the reaction.

We first consider the two conrotatory pathways to **4** as illustrated in Scheme 2. Cleavage of the C1−C6 then C2−C7 bonds leads to **TS1**, for which the C1−C6 bond is 2.5424 Å and the C2−C7 bond is 1.6918 Å. The disparity of the two lengths illustrates the asynchronous nature of the reaction pathway. The C1−C2 and C6−C7 bonds are midway between single and double bond lengths, showing that these two bonds have appreciable double bond character at the transition state. The C6−C7 bond is 0.0261 Å shorter than the C1−C2 bond, which follows from the full cleavage of C1−C6 compared to C2−C7 and that C1−C2 is forming a trans double bond. H1 moves toward the ring early on the potential-energy surface as shown by the 163° H1−C1−C2−H2 dihedral at the transition state. Cleavage of the bond pair in reverse order, C2−C7 then C1−C6, leads to **TS2** which is 2.0 kcal mol^{-1} higher in energy than **TS1**. Noticeable geometric differences include the C1−C2 bond length (cis double bond), which is 0.024 Å longer than that in **TS1**, and the C6−C7 length (trans double bond), which is 0.023 Å longer than the C1−C2 bond in **TS1**. The C1−C6 bond is the second to break in the process, and it is somewhat shorter, by 0.065 Å, in **TS2** than the analogous bond in **TS1**. Overall, it appears that the saddle point for **TS1** is slightly more advanced than that for **TS2**.

The intrinsic reaction coordinates from **TS1** and **TS2** lead to different conformers of **4**, which are separated by 1.5 kcal mol^{-1}. **TS1** leads to the lowest energy isomer **4**, while **TS2** leads to the higher energy isomer **4′**. The main difference between the two conformers is the C4−C5−C6−C7 dihedral, which is 25° in **4** and 81° in **4′**.

The disrotatory pathway proceeds through cleavage of the same bond pairs as the conrotatory mechanism; however, it is much more asynchronous, and two cis double bonds are formed in the diene product (Scheme 3). Cleavage of the C1−C6 then C2−C7 bonds leads to **TS9**, while cleavage of C2−C7 then C1−C6 leads to **TS10**. The C1−C6 length in **TS9** is 2.6011 Å, while the C2−C7 length is 1.5599 Å. The C2−C7 length is 0.1319 Å shorter compared to **TS1**. In addition, the C1−C2 and C6−C7 bonds are substantially longer in **TS9** than in **TS1**, showing that there is not appreciable double bond character yet in the transition state. The H1−C1−C2−H2 dihedral is 14°, indicitave of formation of a cis double bond. As could be expected from these geometrical differences, **TS9** shows substantial biradical character as witnessed by the 1.07 and 0.93 natural orbital occupation numbers for the bonding and antibonding orbitals, comprising the C1−C6 bond, respectively. The activation barrier is 55.0 kcal mol^{-1}, much higher than the 39.5 kcal mol^{-1} value for the allowed conrotatory pathway. Cleavage of the bond pair in reverse order, C2−C7 then C1−C6, results in **TS10** which is 2.0 kcal mol^{-1} in energy above **TS9** giving an activation barrier of 57.0 kcal mol^{-1}. The orbital occupation numbers for the occupied and virtual molecular orbitals for C2−C7 are 1.02 and 0.99, respectively, also illustrating strong configurational mixing in the wave function.

Starting from (*E*,*Z*)-1,3-cycloheptadiene, **4** and **4′**, two pathways exist; conrotatory ring closure to give **2** or rotation of the trans double bond to give **3** as shown in

SCHEME 3

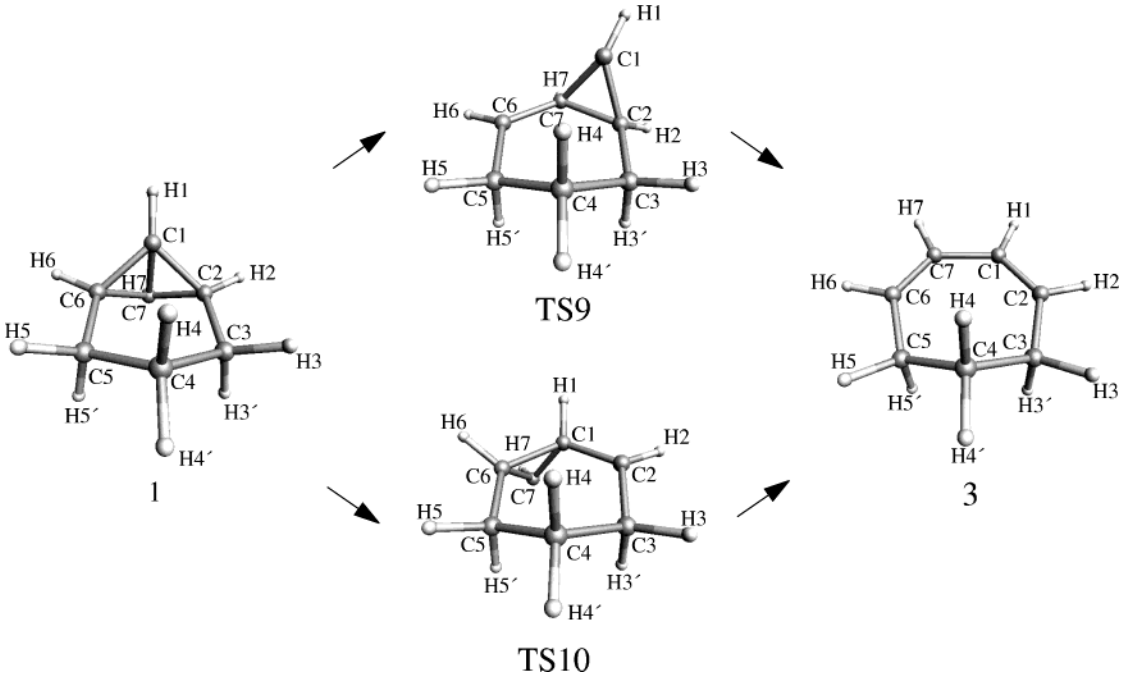

SCHEME 4

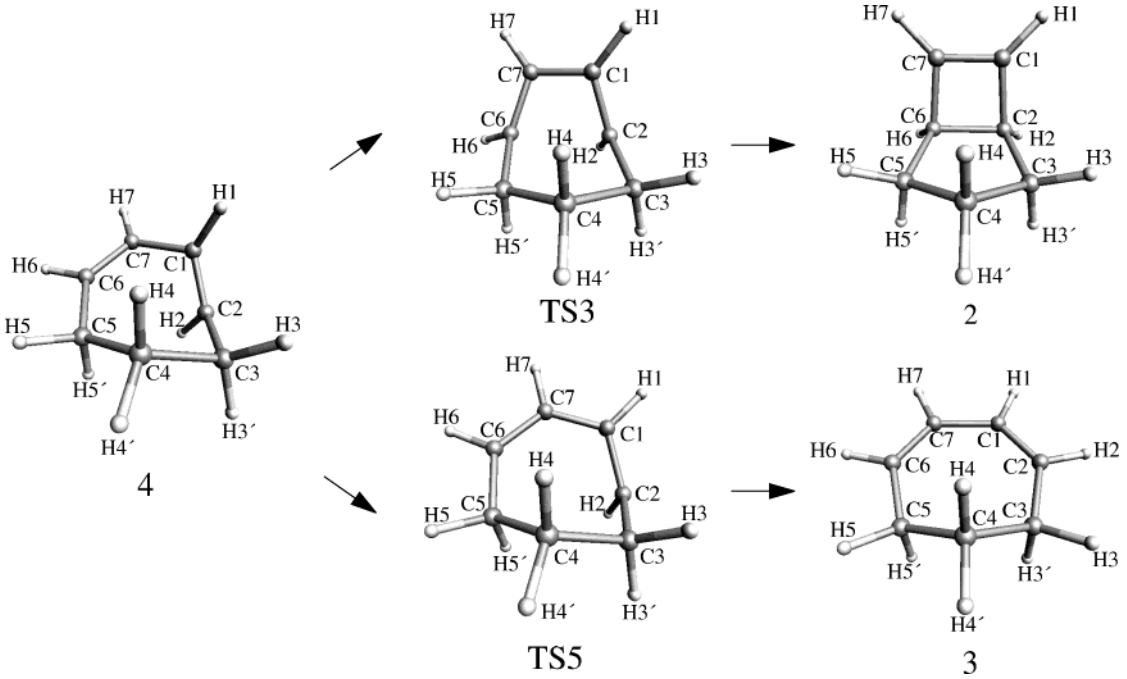

Schemes 4 and 5. **TS3** connects the lowest-energy conformer **4** to the lowest-energy conformer **2**, while **TS4** connects **4′** to **2′**. The conrotatory pathway follows bond formation between C2 and C6 while a double bond forms between C1 and C7. At **TS3**, the C2−C6 length has decreased from 2.7631 Å in **4** to 2.2825 Å. The C1−C7 length has also decreased to 1.3930 Å, close to a double bond. The two double bonds in **4** have increased in length midway between single and double bond distances. The related bonds in **TS4** are similar to those in **TS3**, with the exception of the C4−C5−C6−C7 dihedral, which is 130° larger in **TS4**. The energy difference between **TS3** and **TS4** is only 0.7 kcal mol^{-1}, and the activation barriers are 12.7 and 12.0 kcal mol^{-1} from **4** and **4′**, respectively. The products **2** and **2′** both belong to point group C_s and differ in energy by 4.2 kcal mol^{-1}, with the main structural difference being represented by the C4−C3−C2−C6 dihedral, which is −22.3° in **2** and 23.1° in **2′**, similar to a boat and chair designation.

Conversion of **4** or **4′** directly to **3** can occur through rotation of the trans double bond, through **TS5** and **TS6**, as confirmed by calculation of the intrinsic reaction coordinate for each. The value of the H1−C1−C2−H2 dihedral in **TS5** is −108°, slightly more than a purely orthogonal arrangement. Cleavage of the trans π bond (C1═C2) has caused the C1−C2 length to increase to over

SCHEME 5

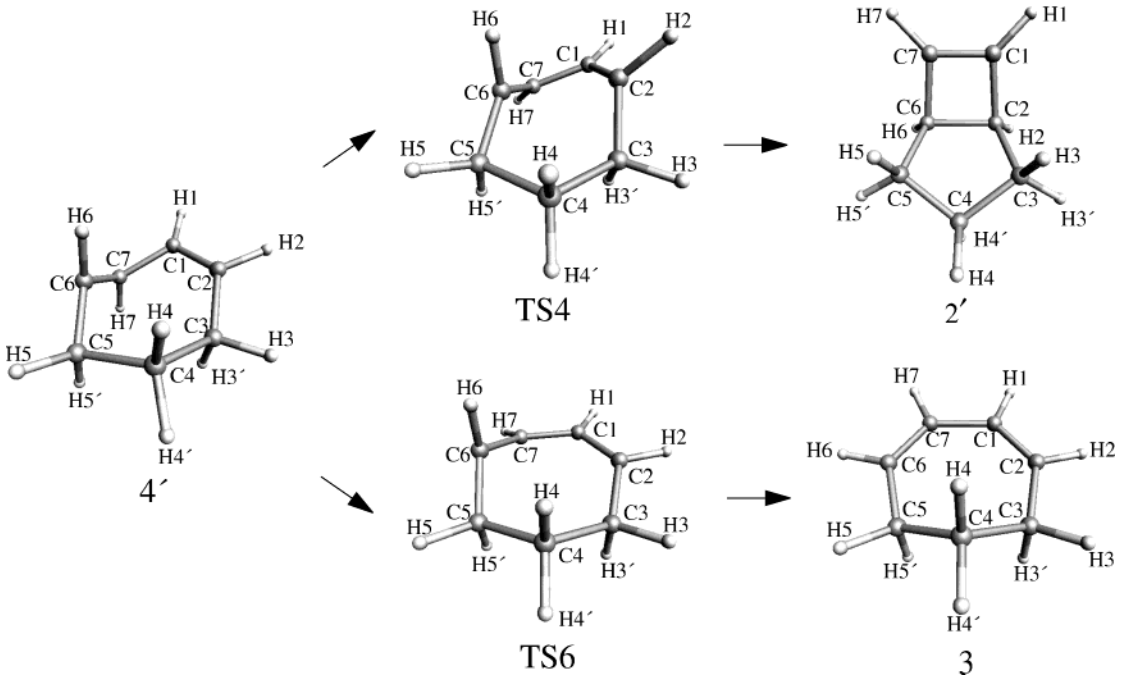

1.5 Å, the C1—C7 length to shrink from 1.5026 to 1.4211 Å, and the C6—C7 to lengthen from 1.3715 to 1.4089 Å. This is indicative of delocalization of an electron from the cleaved π bond with the π electrons from the cis double bond over the C1—C7 and C6—C7 linkages. Similar behavior is seen in **TS6**, resulting from 4′ which is 2.8 kcal mol^{-1} higher in energy than **TS5**. The barrier from **4** to **3** is 19.6 kcal mol^{-1} while that from **4′** is 21.0 kcal mol^{-1}. It is interesting to compare the barriers for π-bond rotation to the six-carbon (*E*,*Z*)-1,3-cyclohexadiene,[5] which has a π-bond rotation barrier of only 2.8 kcal mol^{-1}. The release of a substantial amount of strain for the smaller ring nearly offsets the energy required to rotate the π bond. The transition state also comes earlier on the potential energy surface, as witnessed by a H—C—C—H dihedral (about the trans bond) of 136°. **4** and **4′** are only slightly less strained as the barrier for π-bond rotation is much less than that of unstrained ethylene.

As mentioned above, the thermolysis of **2** gave **3** as the only product, and the activation energies of 45.5 kcal mol^{-1} in the gas phase and 45.9 kcal mol^{-1} in solution were measured.[4] We have calculated barriers for both the conrotatory and disrotatory pathways. The conrotatory (allowed) pathway leads through the intermediate **4** with an **2** → **4** barrier of 35.1 kcal mol^{-1}. The intermediate **4** can then undergo trans π-bond rotation to give **3** with an activation barrier of 19.6 kcal mol^{-1}. As given earlier, the barrier for the reaction of **4** back to **2** is only 12.7 kcal mol^{-1}. Branton et al.[4] stated from their studies that the isomerization of **2** → **3** is strictly first order. Since the **4** → **2** barrier is substantially lower than the **4** → **3** barrier, a **2** ⇄ **4** preequilibrium may be assumed. In this way, an effective first-order rate constant is obtained, and the effective first-order activation barrier becomes simply $E_{a,2\rightarrow4} + E_{a,4\rightarrow3} - E_{a,4\rightarrow2}$. The calculated effective barrier then becomes 42.0 kcal mol^{-1} corresponding to conrotatory ring opening of **2** to give **4** and subsequent π-bond rotation to produce **3**. If the reaction for the structural isomers **2′** ⇄ **4′** → **3** is followed, the barrier is calculated to be 40.6 kcal mol^{-1}.

The disrotatory pathway for **2** → **3** includes the boat form transition-state **TS7**, which links **2** to **3**, while the chair form **TS8** links the higher-energy chair conformer **2′** to **3**. At the transition state, the C2—C6 bond has increased to almost 2.7 Å, but the C1—C7 bond still has double bond character at 1.36 Å. The activation barrier from **2** is 48.2 and 45 kcal mol^{-1} from the higher energy conformer **2′**. The transition states have substantial biradical character with orbital occupation numbers of 1.32 and 0.68 and 1.30 and 0.70 for the occupied and virtual C2—C6 bonds in **TS7** and **TS8**, respectively. Our calculated value for the conrotatory **2** → **3** pathway, including a **2** ⇄ **4** preequilibrium, is 3.5 kcal mol^{-1} below the experimental value, while the calculated barrier for the forbidden disrotatory pathway is 2.9 kcal mol^{-1}above the measured value, making the relative difference between the barriers for the two calculated pathways 6.4 kcal mol^{-1}. However, if the energy difference between the transition states corresponding to the the first step in the conrotatory process (**TS3**) and that for the disrotatory process (**TS7**) is compared, the magnitude is larger at 13.1 kcal mol^{-1}, more in line with the energy difference between **TS1** and **TS9**, the difference for the con- and disrotatory pathways for **1**, at 15.4 kcal mol^{-1}.

Summary and Conclusions

A schematic diagram of the potential-energy surface for isomerization of **1** and **2** is given in Figure 1. The thermal isomerizations of both **1** and **2** have been investigated using multiconfiguration self-consistent field calculations. The lowest energy pathway for each follows an allowed conrotatory process with (*E*,*Z*)-1,3-cycloheptadiene **4** as a common intermediate and **3** as a final product. The thermolysis of both **1** and **2** occurs in two steps, a conrotatory ring opening to **4** and rotation about

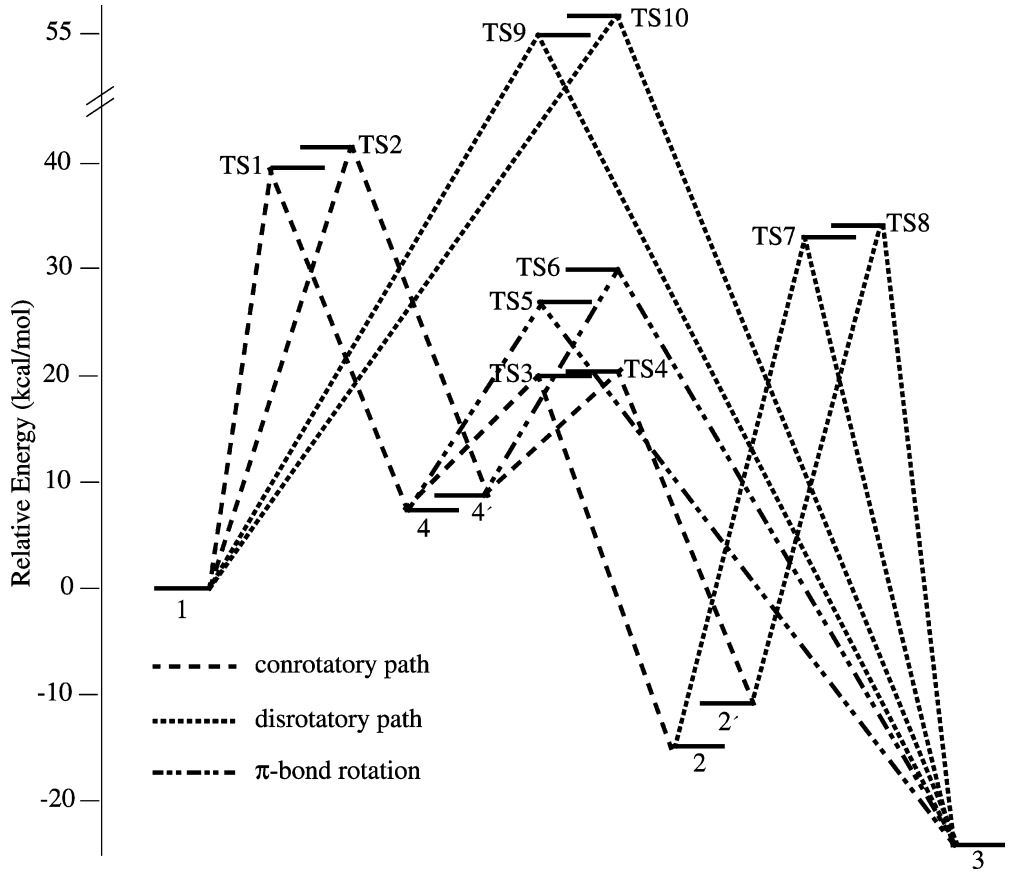

FIGURE 1. Schematics of the MCSCF(10,10) PES(ΔE +ZPE).

SCHEME 6

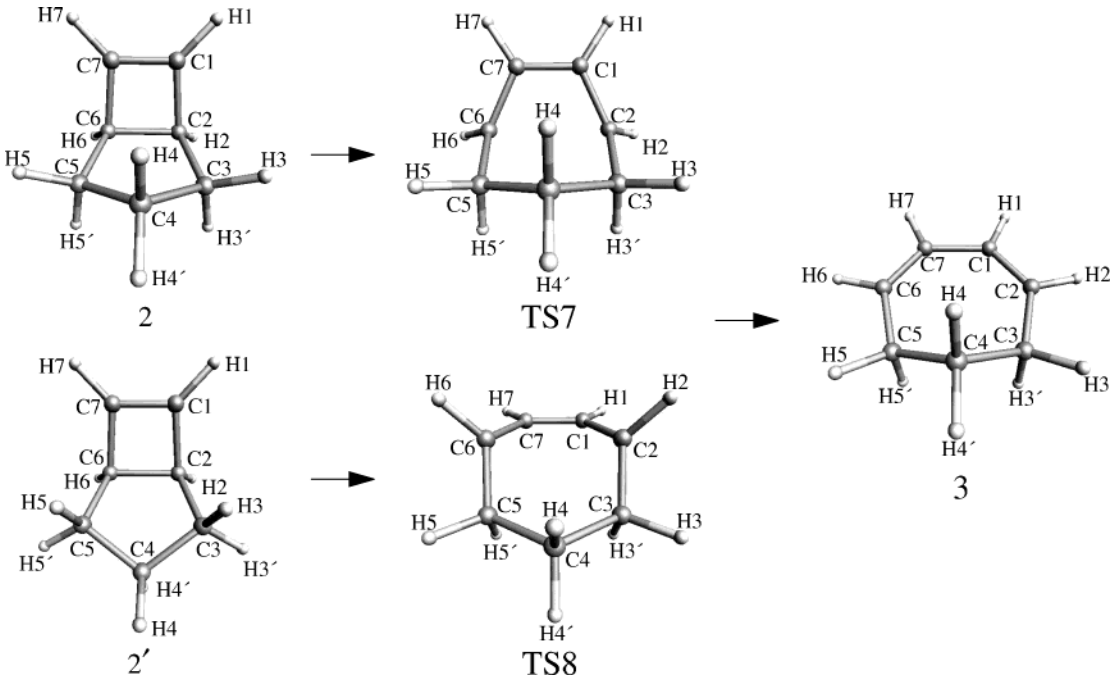

the trans double bond to give **3**. The intrinsic reaction coordinates confirm that **4** is a viable intermediate for the allowed conrotatory pathways. The activation barrier for conversion of **1** → **4** was calculated to be 39.5 kcal mol^{-1}, which agrees well with the 37.6 kcal mol^{-1} experimental value[3] for the conversion of **1** → **2** in solution. The direct route from **1** to **3** is a forbidden disrotatory process and has a much higher activation barrier of 55.0 kcal mol^{-1}. In the isomerization of **2**, if a preequilibrium between **2** and **4** is assumed, the effective first-order activation barrier was found to be 42.0 kcal mol^{-1}, slightly less than the 45.5 kcal mol^{-1} experimental

value. The direct route from **2** to **3** has a barrier of 48.2 kcal mol^{-1}, only 2.7 kcal mol^{-1} higher than the experimental value. The 6.4 kcal mol^{-1} difference in the allowed and forbidden pathways is not that great; however, the initial barrier of the allowed **2** → **4** step, at 35.1 kcal mol^{-1}, is much smaller than the 48 kcal mol^{-1} barrier for the forbidden step, making the former the preferred pathway. Starting from the intermediate **4**, since **TS3** is lower in energy than **TS5**, the formation of **2** is favored over that for **3**, making the comment by Wiberg et al.[1] that **3** is formed from **2** correct.

The relative energies calculated at the MCSCF and MCQDPT2 levels are compared in Tables 1 and 3. Inclusion of electron correlation outside the active space turned out to have a large effect on the relative energies, as detailed previously.[19−20] With the selection of **1** as the zero energy reference, the relative energy differences for **2** and **2′** are 4 and 5 kcal mol^{-1}, respectively, and approximately 8 kcal mol^{-1} for **4** and **4′**. The largest difference is for **3**, in which a 14 kcal mol^{-1} difference is shown. We were concerned that convergence of the perturbation expansion might be in question, so we calculated the relative energies at the CCSD(T) level, using the same basis set. Since only the wave functions for the transition states show significant configurational mixing, a single-determinant wave function for the minima structures is adequate. The relative energies calculated at the MCQDPT2 and CCSD(T) levels are reasonably close together; therefore we feel confident in the relative energies resulting from the MCQDPT2 level. Although we are not able to explicitly confirm theseholds for the transition states, the activation barriers are consistent with experimental values.

Acknowledgment. The authors gratefully acknowledge the National Science Foundation, through the EPSCoR program, for finacial support and the Mississippi Center for Supercomputing Research for computing time.

Supporting Information Available: Cartesian coordinates and selected internal coordinates for each structure (minima and transition states) along with intrinsic reaction coordinate plots for each transition state are available as Supporting Information in PDF file. This material is available via the Internet at http://pubs.acs.org.

JO035168S

(19) Borden, W. T.; Davidson, E. R. *Acc. Chem. Res.* **1996**, *29*, 67.
(20) Hrovat, D. A.; Morokuma, K.; Borden, W. T. *J. Am. Chem. Soc.* **1994**, *116*, 1072.